Telomerase-Mediated Strategy for Overcoming Non–Small Cell Lung Cancer Targeted Therapy and Chemotherapy Resistance

Ilgen Mender[*], Ryan LaRanger[*], Krishna Luitel[*], Michael Peyton[†], Luc Girard[†,‡,§], Tsung-Po Lai[*], Kimberly Batten[*], Crystal Cornelius[*], Maithili P. Dalvi[†], Michael Ramirez[¶], Wenting Du[‡], Lani F. Wu[#], Steven J. Altschuler[#], Rolf Brekken[‡,**], Elisabeth D. Martinez[†,‡,§], John D. Minna[†,‡,§,**], Woodring E. Wright[*,††] and Jerry W. Shay[*]

[*]Department of Cell Biology, University of Texas Southwestern Medical Center, Dallas, TX 75390, USA; [†]Hamon Center for Therapeutic Oncology Research, University of Texas Southwestern Medical Center, Dallas, TX 75390, USA; [‡]Department of Pharmacology, UT Southwestern Medical Center, Dallas, TX 75390, USA; [§]Simmons Comprehensive Cancer Center, UT Southwestern Medical Center, Dallas, TX 75390, USA; [¶]Green Center for Systems Biology, University of Texas Southwestern Medical Center, Dallas, TX 75390, USA; [#]Department of Pharmaceutical Chemistry, University of California, San Francisco, California 94158, USA; [**]Division of Surgical Oncology, Department of Surgery and Hamon Center for Therapeutic Oncology Research, UT Southwestern Medical Center, Dallas, TX; [††]Department of Internal Medicine, UT Southwestern Medical Center, Dallas, TX 75390, USA

Abstract

Standard and targeted cancer therapies for late-stage cancer patients almost universally fail due to tumor heterogeneity/plasticity and intrinsic or acquired drug resistance. We used the telomerase substrate nucleoside precursor, 6-thio-2′-deoxyguanosine (6-thio-dG), to target telomerase-expressing non–small cell lung cancer cells resistant to EGFR-inhibitors and commonly used chemotherapy combinations. Colony formation assays, human xenografts as well as syngeneic and genetically engineered immune competent mouse models of lung cancer were used to test the effect of 6-thio-dG on targeted therapy– and chemotherapy-resistant lung cancer human cells and mouse models. We observed that erlotinib-, paclitaxel/carboplatin-, and gemcitabine/cisplatin-resistant cells were highly sensitive to 6-thio-dG in cell culture and in mouse models. 6-thio-dG, with a known mechanism of action, is a potential novel therapeutic approach to prolong disease control of therapy-resistant lung cancer patients with minimal toxicities.

Neoplasia (2018) 20, 826–837

Introduction

Lung cancer is the most common cause of cancer-related deaths [1]. However, tumor acquired drug resistance is one of the major reasons why chemotherapy and targeted therapies fail to provide durable responses [2, 3]. Almost universally, tumors develop resistance due to intratumor heterogeneity and/or different mechanisms such as target gene alterations (i.e., amplification of epidermal growth factor

receptor [EGFR] and EGFR T790M mutation), downstream bypass signaling pathway activation (i.e., MET amplification or BRAF mutations), and phenotypic alterations (epithelial to mesenchymal transition), thus limiting the success of targeted therapies in lung cancer [4,5]. Osimertinib (AZD9291) is an FDA-approved EGFR inhibitor which is used to overcome drug resistance in non–small cell lung cancer (NSCLC) with the EGFR T790M mutation. Despite the impressive results of this drug, acquired resistance still develops, and little is known about drug resistance mechanisms [6]. In addition, there are diverse erlotinib resistance mechanisms that can emerge in what is termed "persister" derived resistant clones that arise from a single cell [7], indicating the complexity of resistance mechanisms. Likewise, while subsets of lung cancer patients have durable responses to checkpoint inhibitors, in the majority of cases, resistance also develops [8]. Thus, for all types of lung cancer systemic treatment modalities, there remains an outstanding need to develop new approaches to treat resistant tumors including biomarkers predictive signatures of response to any new treatment modalities to prolong disease control.

Telomerase is an almost universal biomarker in advanced human cancers [9,10]. Telomerase inhibitors are a potentially important class of targeted therapies; however, long-duration treatments result in hematological toxicities that prevent their advancement in clinical use. For example, a lead telomerase oligonucleotide, imetelstat (IMT), has not progressed well in clinical trials due to a long lag period to observe clinical benefit and drug-related hematological toxicities [11,12]. When IMT therapy is temporarily stopped, tumor telomerase is immediately reactivated and tumor telomeres rapidly regrow [13]. Thus, finding alternative strategies to target telomerase positive cancer cells is an urgent need.

6-thio-2′-deoxyguanosine (6-thio-dG), a modified nucleoside, is preferentially incorporated into telomeres but only in telomerase-positive cells [14]. When an altered nucleotide, 6-thio-dG, is incorporated into the telomere sequence, it leads to rapid telomere uncapping, genomic instability, and cell death. Therefore, while 6-thio-dG rapidly kills the telomerase-positive cancer cells, it has minimal effects on telomerase-negative normal cells. Additionally, we found that 6-thio-dG induced no significant toxicity in mice (no weight loss; no changes in hematological, renal, or liver functions) [14,15]. This led us in the current study to test the effect of 6-thio-dG on lung cancers that are resistant to platin-doublet chemotherapy or EGFR tyrosine kinase inhibitor–targeted therapies. We find that cells resistant to first-line standard chemotherapies or EGFR-targeted therapies remain sensitive to 6-thio-dG treatment at pharmacological doses. Together, our observations suggest that 6-thio-dG may be an effective therapeutic approach to prolong disease control in therapy-resistant tumors.

Materials and Methods

Cell Lines

The NCI and HCC lung cancer lines used were obtained from the UT Southwestern Hamon Center repository. Except when noted, NSCLC cell lines were grown in a Medium X (DMEM:199, 4:1, Hyclone, Logan, UT) supplemented with 10% cosmic calf serum (Hyclone, Logan, UT) without antibiotics and incubated in a humidified atmosphere with 5% CO_2 at 37°C. NSCLC cell lines were authenticated using the Power-Plex 1.2 kit (Promega, Madison,

WI) and confirmed to match the DNA fingerprint library maintained by ATCC and confirmed to be free of mycoplasma by e-Myco kit (Boca Scientific, Boca Raton, FL). Human bronchial epithelial cells (HBECs) were cultured in bronchial epithelial growth medium (Lonza, Allendale, NJ) with an antibiotic solution (penicillin G–streptomycin–amphotericin B) and incubated in low oxygen (2%-3%) at 37°C. PC9-derived erlotinib-sensitive (PC9-1) and erlotinib-resistant clones [persister-derived erlotinib-resistant clone (PERC)9, PERC10, PERC13, PERC16, PC9-ER] were generated as previously described [7]. These cells were grown in RPMI-1640 (Sigma, St Louis, MO) supplemented with 5% fetal bovine serum (Hyclone, Logan, UT) without antibiotics. H1299 parental cells were treated long term with increasing doses of paclitaxel+carboplatin combination (2:3 ratio) to generate H1299 paclitaxel/carboplatin-resistant cells. Surviving cells were cultured in drug-free media until they repopulated the plate (one cycle); then a second treatment cycle was started. After 18 repetitive cycles of treatment, H1299 T18 paclitaxel/carboplatin-resistant cells were generated [16].

Drug Preparation

For in vitro studies, 6-thio-dG (Metkinen Oy, Kuopio, Finland) was dissolved in DMSO/water (1:1) to prepare 10 mM stock solutions, which were kept frozen at –20°C. A 1 mM, final concentration stock was prepared for in vitro experiments and added in fresh medium at different concentrations. Erlotinib HCl (Selleckchem, Houston, TX) was dissolved in DMSO to prepare 10 mM stock solutions, which were kept frozen at –80°C. A 2.5 μM erlotinib final concentration was used for in vitro experiments. Osimertinib and paclitaxel (Selleckchem) were dissolved in DMSO, and carboplatin (Selleckchem) was dissolved in water to prepare 10 mM stock solutions, which were kept frozen at –80°C. A 1 mM final concentration stock was prepared for in vitro experiments and added in fresh medium at different concentrations.

For mouse in vivo studies, 6-thio-dG was prepared in 5% DMSO for intraperitoneal (i.p.) injection or 0.4% (hydroxypropyl)methyl cellulose (Sigma, Saint Louis, MO) for oral gavage. Erlotinib was prepared in 15% Captisol (β-cyclodextrin, sulfobutyl ethers, sodium salts) (Cydex Pharmaceuticals, Lawrence, KS) for oral gavage. Gemcitabine HCl and cisplatin (Selleckchem) were dissolved in 0.9% NaCl saline solution for i.p. injections.

Cell Viability Assay

For IC_{50} determinations, a panel of NSCLC cell lines was screened with 6-thio-dG with a four-fold dilution series in 8 different points in 96-well plates. Cells were plated 24 hours prior to addition of drug, incubated for 4 days, and assayed using MTS (CellTiter 96 Aqueous One Solution Cell Proliferation Assay) according to the manufacturer's instructions (Promega). Cell number per well ranged from 500 to 4000 cells per well inversely proportional to doubling times (typically 2000/well). Dose-response curves were generated and IC_{50} calculated using in-house software DIVISA. All samples were analyzed in triplicate, and standard deviations are from two to three independent experiments.

For determination of viable cells with cell counting, normal HBEC cells (10,000 cells/cm^2) were treated with 6-thio-dG (1, 3, 10 μM) every 3 days for 2 weeks. The cells were counted at the end of first week and replated for a second week. H1299 parental (800 cells/cm^2) and T18 (1600 cells/cm^2) cells were grown in a Medium X (DMEM:

199, 4:1, Hyclone, Logan, UT) supplemented with 10% cosmic calf serum (Hyclone) without antibiotics and treated with 6-thio-dG (1, 3, 10 μM) every 3 days for 1 week.

For combination treatment of IMT and 6-thio-dG, H2087 cells (3750-5000 cells/cm^2) were seeded into six-well plates. After cell attachment (next day), 5 μM IMT was added in fresh medium (pretreated). Three days later, either 5 μM IMT or 1 μM 6-thio-dG or combination of IMT (5 μM) and 6-thio-dG (1 μM) was added in fresh medium and cultured for 3 days.

Colony Formation Assay

PC9-1 and PERCs (PERC9, PERC10, PERC13, PERC16, and PC9-ER) were seeded in three different concentrations on six-well plates (250-4000 cells/ well) in erlotinib or erlotinib-free medium and treated with various drug concentrations every 3-4 days. KLN205, a mouse lung squamous cancer cell line obtained from the American Type Culture Collection (CRL-1453) [17], was seeded in three different concentrations in six-well plates (1000-4000 cells/well) and treated with various drug concentrations every 3-4 days. H1299 parental and T18 cells were seeded in three different concentrations on six-well plates (400-1000 cells/well) and treated with various drug concentrations every 3-4 days. Following 11-13 days of treatment, cells were fixed and stained with 6% glutaraldehyde (Fisher Scientific, Pittsburgh, PA) plus 0.5% crystal violet (Sigma) solution. After washing with tap water, cells were air-dried and images were captured using a G-BOX (Syngene, model: G-BOX F3).

Droplet Digital TRAP Assay (Telomerase Activity)

Quantitation of telomerase enzyme activity was performed as described in [18].

Telomere Dysfunction-Induced Foci (TIF) Assay

The TIF assay is based on the colocalization detection of DNA damage by an antibody against DNA damage response factors such as gamma-H2AX, 53BP1, and telomeres using FAM-conjugated telomere sequence (C-rich)–specific peptide nucleic acid (PNA) probe. Briefly, cells were seeded into four-well chamber slides, and after the cells attached (next day), slides were rinsed twice with phosphate-buffered saline (PBS) and fixed in 4% formaldehyde (ThermoScientific, IL) in PBS for 10 minutes. Then, cells were washed twice with PBS and permeabilized in 0.5% Triton X-100 in PBS for 10 minutes. Following permeabilization, cells were washed three times with PBS. Cells were blocked with 10% goat serum in 0.1% PBST (TritonX-100) for 1 hour. Gamma-H$_2$AX (mouse) (Millipore, Billerica, MA) was diluted 1:1000 in blocking solution and incubated on cells for 2 hours. Following three washes with PBST (1× PBS in 0.1% Triton) and three washes with PBS, cells were incubated with Alexaflour 568–conjugated goat anti-mouse (1:500) (Invitrogen, Grand Island, NY) for 40 minutes and then washed five times with 0.1% PBST. Cells were fixed in 4% formaldehyde in PBS for 20 minutes at room temperature. The slides were sequentially dehydrated with 70%, 90%, and 100% ethanol followed by denaturation with hybridization buffer containing FAM-conjugated telomere sequence (C-rich)–specific PNA probe (PNA Bio, Thousand Oaks, CA), 70% formamide, 30% 2× SSC, 10% (w/v) MgCl$_2$.6H$_2$O (Fisher Sci), and 0.25% (w/v) blocking reagent for nucleic acid hybridization and detection (Roche) for 7 minutes at 80°C on a heat block, followed by overnight incubation at room temperature. Slides were washed sequentially with 70% formamide (Ambion, Life

Technologies, Grand Island, NY)/0.6× SSC (Invitrogen) (2 × 1 hour), 2× SSC (1 × 15 minutes), and PBS (1 × 5 minutes); sequentially dehydrated with 70%, 90%, and 100% ethanol; and then mounted with Vectashield mounting medium with DAPI (Vector Laboratories, Burlingame, CA). Images were captured with a Deltavision wide-field microscope using the 60× objective. TIFs were quantified as previously described [19].

Establishment of Xenograft Models

Animal experiments were approved (APN 2016-101375) by the University of Texas Southwestern Institutional Animal Care and Use Committee and conducted as per institutional guidelines. A subcutaneous xenograft mouse model of the human PC9-1 and PERC16 NSCLC cell lines was used to evaluate the effects of erlotinib and 6-thio-dG treatment *in vivo*. Athymic NCR nu/nu female mice (~6 weeks old) were used (Charles River, Wilmington, MA). A total of 2×10^6 PC9-1 and 4×10^6 PERC16 cells were inoculated subcutaneously into the left and right dorsal flanks of nude mice in 100 μl PBS. When tumors became visible, mice were divided into control, 6-thio-dG, and erlotinib treatment groups. In the PC9-1 group, control mice were intraperitoneally injected with a DMSO/PBS mixture, while in the experimental group, animals were injected with 6-thio-dG (5 mg/kg, i.p.) or given erlotinib (15 mg/kg, oral gavage) every day for 15 days in 100 μl drug solution per mouse. In the PERC16 group, control mice were intraperitoneally injected DMSO/PBS mixture for 12 days and then given 0.4% (hydroxypropyl)methyl cellulose as oral gavage for 1 week. In the PERC16 experimental group, animals were injected with 6-thio-dG (5 mg/kg, i.p.). Another group was given erlotinib (15 mg/kg, oral gavage) every day for 12 days and then switched to 6-thio-dG (5 mg/kg, oral gavage) for 1 week in 100 μl drug solution per mouse.

A subcutaneous xenograft mouse model was used to evaluate the effects of 6-thio-dG treatment on paclitaxel/carboplatin-resistant H1299 T18 NSCLC *in vivo*. Athymic NCR nu/nu female mice (~6 weeks old) were used (Charles River). A total of 3×10^6 H1299 T18 cells were inoculated subcutaneously into the left and right dorsal flanks of the nude mice in 100 μl PBS. When tumors became visible (~50mm^3), mice were divided into control (DMSO/PBS, i.p., daily) and 6-thio-dG treatment groups (5 mg/kg, i.p., daily).

A syngeneic tumor mouse model was used to evaluate the effects of combination therapy of 6-thio-dG *in vivo*. DBA/2 female mice (~6-8 weeks old) were used (Charles River). A total of 3.6×10^5 KLN205 cells were inoculated subcutaneously into the left and right dorsal flanks of the DBA/2 mice in 100 μl PBS. When tumors became visible, mice were divided into control, 6-thio-dG, gemcitabine + cisplatin, and gemcitabine + cisplatin + 6-thio-dG treatment groups. The following concentrations were used for 6-thio-dG, gemcitabine, and cisplatin: 2.5 mg/kg (oral gavage, daily), 15 mg/kg (i.p., every 2-3 days), and 1 mg/kg (i.p., every 5-6 days), respectively. The group that was given gemcitabine + cisplatin doublet therapy for 13 days was switched to 6-thio-dG alone (5 mg/kg, i.p.) for 2-4 days at the end of treatment in 100 μl drug solution per mouse. Animals were weighed every other day during the treatment period. Tumor volumes were measured by calipers and recorded every 2 days. Tumor volumes were calculated by taking the length to be the longest diameter across the tumor and width to be the corresponding perpendicular diameter using the following formula: (length × width^2) × 0.5. The animals were sacrificed by CO$_2$ inhalation 24 hours after the last dose of treatment.
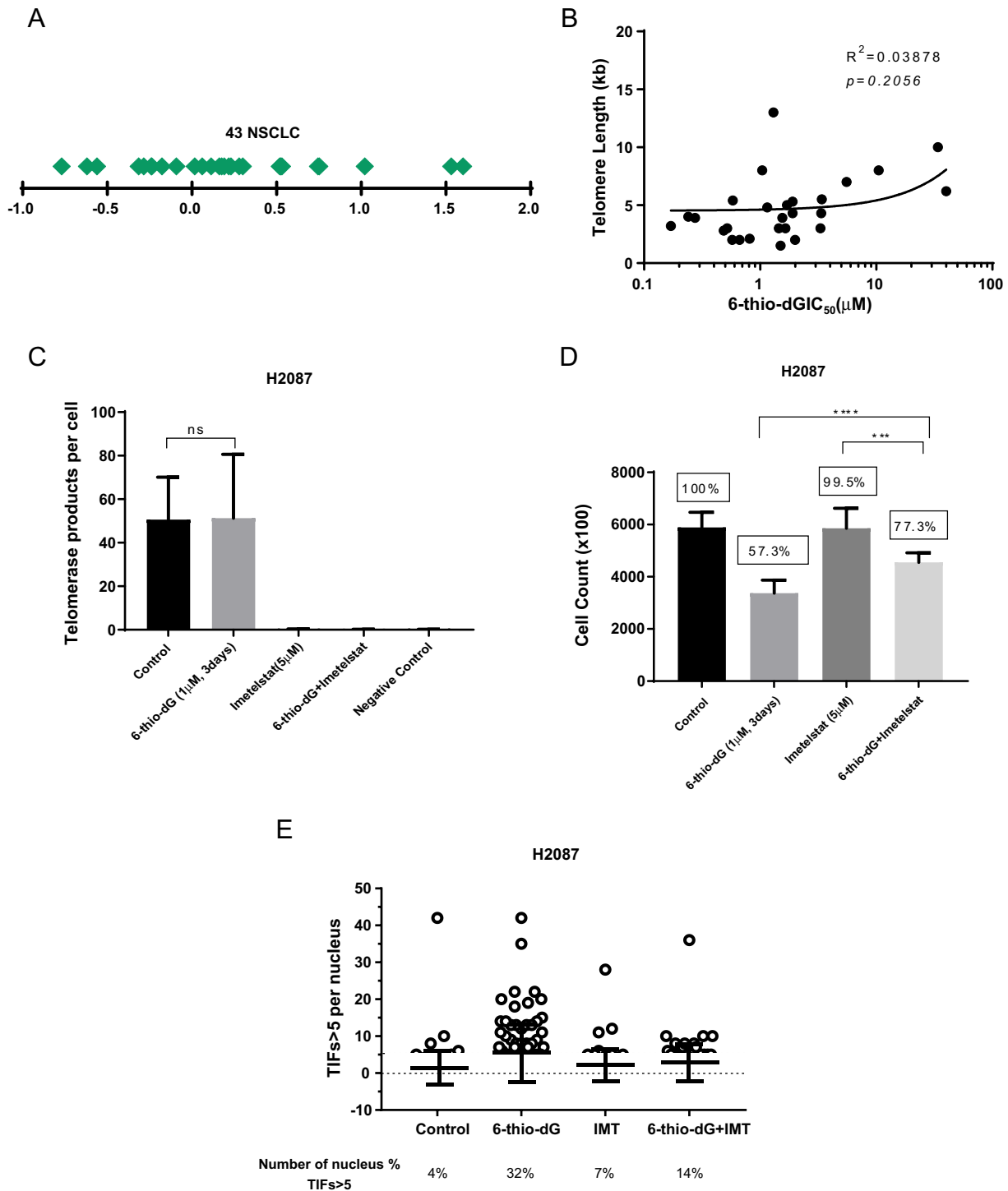
Figure 1. (A) Column scatter graph shows the IC_{50} values of NSCLC cells on log10 scale following 6-thio-dG treatment. (B) Lack of correlation between initial telomere length and 6-thio-dG IC_{50} values of NSCLC lines (R^2: 0.03878, P = .2056). (C) ddTRAP assay confirms telomerase inhibition upon IMT treatment in H2087 NSCLCs but no inhibition upon 6-thio-dG treatment. Cells treated with vehicle or 6-thio-dG (1 μM, 3 days) or IMT (5 μM, 6 days) or combination of IMT and 6-thio-dG (pretreated with 5 μM IMT 6 days and then 6-thio-dG 3 days). Negative control: DEPC water (SDs from three independent experiments, control versus 6-thio-dG: P = ns, two-tailed unpaired t test). (D) The cell counts of H2087 NSCLCs treated with either vehicle or 6-thio-dG (1 μM, 3 days) or IMT (5 μM, 6 days) or combination of IMT and 6-thio-dG (pretreated with 5 μM IMT and then 6-thio-dG 3 days) (n = 7-9, pooled from three independent experiments, two-tailed unpaired t test, ***P = .0005, ****P < .0001). (E) TIF assay confirms induction of TIFs with 6-thio-dG treatment (1 μM, 3 days) and the reduction of TIFs when the cells were pretreated with IMT (5 μM). TIF > 5: cells that have more than 5 TIFs in the nucleus. n = 95 (control). n = 95 (6-thio-dG), n = 57 (IMT), n = 70 (6-thio-dG + IMT). Two-tailed unpaired t test, control versus 6-thio-dG: ****P < .0001, control versus IMT: ns, 6-thio-dG versus 6-thio-dG + IMT: *P = .0105, IMT versus 6-thio-dG + IMT: ns. Supplemental data associated with this figure can be found in Supplemental Fig. S1.

Genetically Engineered Mouse Tumor Model (KRAS^LA1)

Genetically Engineered Mouse Tumor Model (KRAS^{LA1})

This mouse tumor model with an activated oncogenic allele of K-ras has been previously described [20]. The mice were inbred onto 129S2

mice. Germline transmission of the mutant allele (G12D) was confirmed by PCR of tail DNA. KRAS^{LA1} mice were divided into two different groups, and five mice were used for each group. Treatment
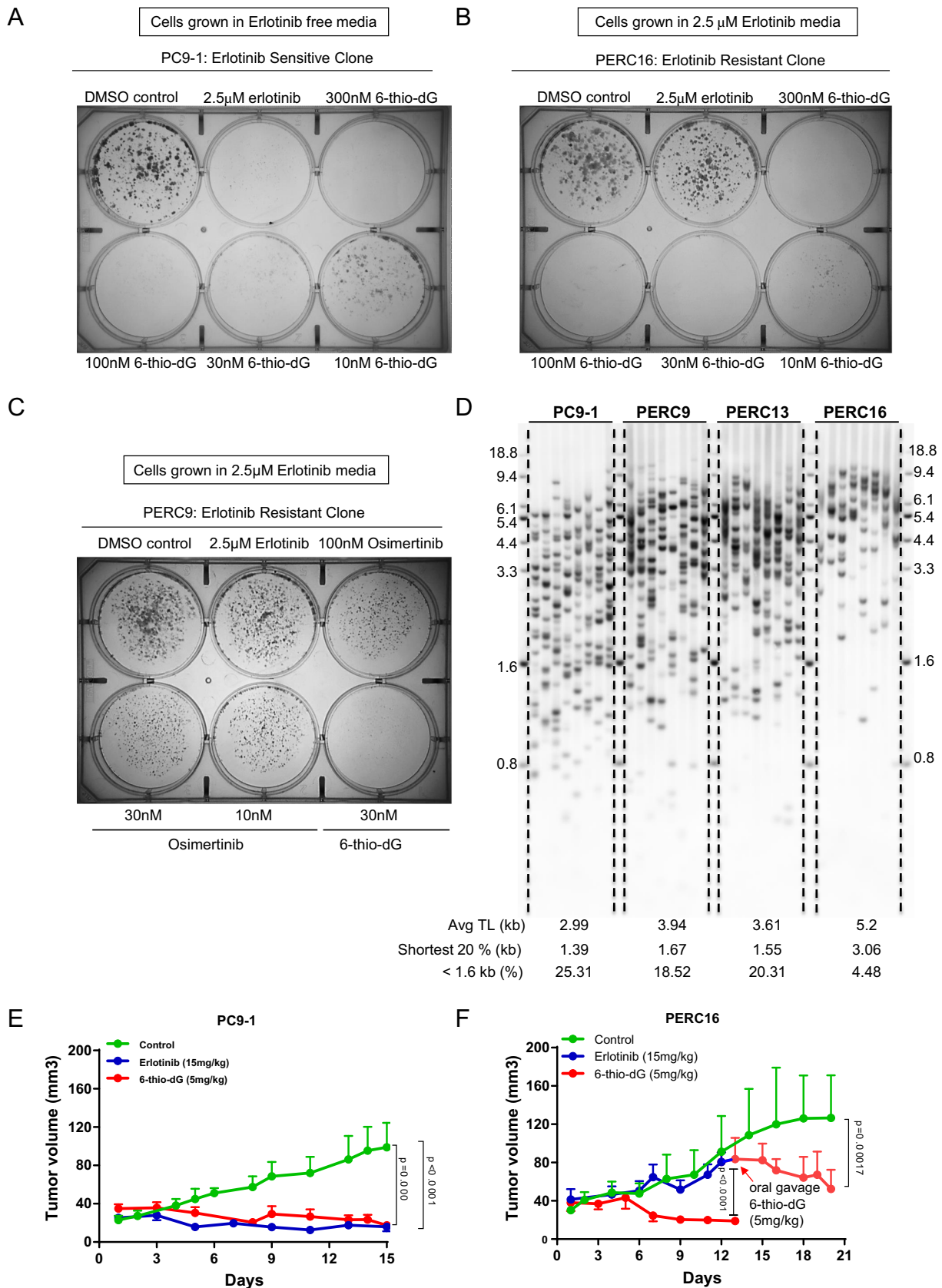
(5% DMSO or 5 mg/kg 6-thio-dG) was started when mice were ~300 days old and continued every day for 14 days (i.p.). The animals were sacrificed by CO_2 inhalation 24 hours after the last dose of treatment. Formalin-fixed, paraffin-embedded tissue was sectioned (5 µm thick), deparaffinized, and stained with hematoxylin I and eosin Y (Fisher Scientific). Surface area (R^2) of neoplastic lesions was measured by using Nanozoomer digital pathology software. Neoplastic lesions were accepted as spheres. Tumor volumes were calculated by using the following formula: $4/3 \cdot \pi \cdot R^3$. Three sections were used for each sample, and each section was 25 µm apart from each other.

Telomere Shortest Length Assay (TeSLA)

The TeSLA was performed as described in [21] to measure the average and the shortest telomere lengths.

Statistical Analysis

Unless otherwise indicated, all data are presented as mean values ± standard deviation (SD) for at two to three replicates. KLN205 tumor volumes in each group were normalized to day 1 measurement in its own group, and therefore, graphs are shown as percentages. Significant differences between experimental conditions were determined using two-tailed, unpaired Student's t test (*$P < .05$, **$P < .005$, ***$P < .0005$, ****$P < .0001$, ns: $P > .05$). ANOVA mixed-effect models were used to determine the differences between control and treatment groups for the time-dependent *in vivo* experiments (tumor growth data) by using R version 3.4.1 and the nlme package. Graphs and other statistical analysis were done using GraphPad Prism software version 7.

Results

Telomerase Dependency on Cell Killing Effects of 6-thio-dG for NSCLC and HBECs

In our previous study, we showed that 6-thio-dG induces apoptosis in telomerase-positive HeLa cervical cancer, pediatric brain tumor (MB004, CCHMC-DIPG1), and melanoma cell lines (A375 and LOX-IMVI BR) [22,23]. In this study, we determined the drug response phenotypes across a panel ($n = 43$) of NSCLC lines representing a wide variety of lung cancer oncogenotypes; response phenotypes to clinically available drugs; and NSCLCs derived from current, former, and lifetime never smokers. We tested these 43 different NSCLC lines in 96-well plates and assayed with 8 different concentrations of 6-thio-dG over a 4-day period to determine IC_{50} values. We found a range of 6-thio-dG IC_{50} values with a large proportion having IC_{50} values in the nanomolar to low micromolar concentration (Figure 1A and Supplementary Fig. S1A). The IC_{50} values for 6-thio-dG in the NSCLC lines as expected were independent of their initial telomere length (Figure 1B). In order to test if the cell killing effects were telomerase dependent, we selected 6-thio-dG–sensitive cell line H2087 and pretreated cells with the telomerase inhibitor IMT, and then continued drug treatment with a combination of IMT and 6-thio-dG to see if the cells would be rescued from 6-thio-dG toxicity (Figure 1, C and D). While IMT treatment (5 µM, 3 days) almost completely inhibited telomerase activity with minimal effect on cell growth, 6-thio-dG (1 µM, 3 days) did not inhibit telomerase activity in H2087 cells (Figure 1C) but had a substantial and quick effect on cell viability (Figure 1D). We observed that while 1 µM 6-thio-dG killed ~45% of the cells in 3 days, short-term treatment with IMT did not affect cell growth rates. However, pretreatment with IMT partially rescued the cell-killing effect of 3 days of 6-thio-dG treatment. However, a subset (~22%) of the cells was still sensitive to 6-thio-dG even in the presence of IMT (Figure 1D).

One explanation is that even the very low residual telomerase activity in the cells after IMT treatment leads to some 6-thio-dG incorporation into telomeres in a subset of cells. To determine if this explanation was correct, we determined the presence of TIF under these conditions and found that 6-thio-dG induces TIFs (32% of cells treated with 6-thio-dG alone have more than 5 TIFs in the nucleus after 72 hours) correlating with cell-killing effect, while inhibition of telomerase with IMT reduced the occurrence of TIFs (14% of the cells treated with 6-thio-dG after IMT treatment that have more than 5 TIFs in the nucleus) (Figure 1E) and rescued most of the cells from 6-thio-dG–induced cell death. This suggests that TIFs may trigger 6-thio-dG–induced cell death (Figure 1, D-E). We used primary cultures of HBECs that are telomerase silent to test the toxicity of 6-thio-dG on telomerase-negative cells and observed minimal cell growth inhibition effects with treatment over a 2-week period (supplementary Fig. S1, B and C). Our previous studies also showed that human normal fibroblasts, colonic epithelial cells, skin keratinocytes, skin melanocytes, and skin fibroblasts are not as sensitive to 6-thio-dG as telomerase-positive cancer cells and 6-thio-dG causes G2/M arrest in telomerase-positive cells with negligible effect in telomerase-negative cells [14,22,23]. These results are consistent with the proposed mechanism of action of 6-thio-dG indicating that expression of telomerase in cells increases the sensitivity to 6-thio-dG with minimal effect on normal cells. In addition, it is possible that genomic damage observed in normal cells may lead to a senescence-like state that may be reversible.

Figure 2. (A) Colony formation assay of erlotinib-sensitive (PC9-1) and (B) -resistant (PERC16) cells that were treated with erlotinib or 6-thio-dG at indicated doses for 11-13 days. (C) Colony formation assay of PERC9 erlotinib-resistant cells that were treated with erlotinib, osimertinib, or 6-thio-dG at indicated doses for 11-13 days. Cells were then fixed and stained with crystal violet. Representative image of three to five biological replicates was shown for each experimental sample. (D) Results of TeSLA using DNA for PC9-1, PERC9, PERC13, and PERC16. Eight TeSLA PCRs (30 pg of each reaction) were performed for each DNA sample. TeSLA image quantification software was used to determine the average telomere length (Avg TL, kb), shortest 20% (kb), and <1.6 kb (%). P .01, fold change 2. (E-F) Intraperitoneal injection or oral gavage of 6-thio-dG in PC9-1– and PERC16-derived xenografts. A total of 15 mg/kg erlotinib (oral gavage) or 5 mg/kg 6-thio-dG (i.p.) was daily given to the PC9-1–derived mice for 15 days. A total of 15 mg/kg erlotinib (oral gavage) or 5 mg/kg 6-thio-dG (i.p.) was daily given to the PERC16-derived mice for 12 days. Following 12 days of erlotinib treatment, 5 mg/kg 6-thio-dG treatment alone was continued to be given orally every day for 1 week. Data in these figures were presented as mean values ± standard error of the mean ($n = 3$-6) (control versus erlotinib: $P < .0001$, erlotinib versus 6-thio-dG: $P = .01$, control versus 6-thio-dG: P = .000 in Figure 2E; control versus erlotinib: $P = .043$, erlotinib versus 6-thio-dG: $P < .0001$, control versus 6-thio-dG: $P < .0001$, comparison for days 12-20 between control versus 6-thio-dG oral gavage: $P = .00017$ in Figure 2F; ANOVA mixed-effect models.). Supplemental data associated with this figure can be found in Supplemental Figs. S2 and S3.

The Effect of 6-thio-dG Therapy on NSCLC Lines Resistant to EGFR Tyrosine Kinase Targeted Therapy or to Platin-Taxane Doublet Chemotherapy

It has been shown that EGFR mutant PC9 NSCLCs are sensitive to the EGFR inhibitor erlotinib, with only 0.5% of cells entering into what is termed a persister state, in which cells initially show little to no cell growth [24]. However, following long-term treatment with 2.5 µM erlotinib, persister clones start regrowing and become resistant to erlotinib. In a previous study, a clone of PC9 (PC9-1) was established from the main population of PC9 cells to reduce the preexisting
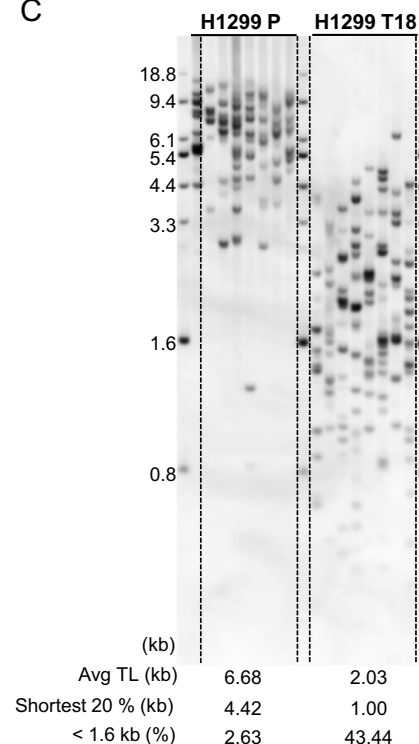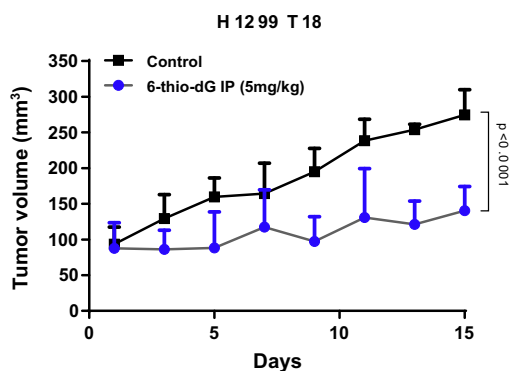
A

B

C

	H1299 P	H1299 T18
Avg TL (kb)	6.68	2.03
Shortest 20 % (kb)	4.42	1.00
< 1.6 kb (%)	2.63	43.44
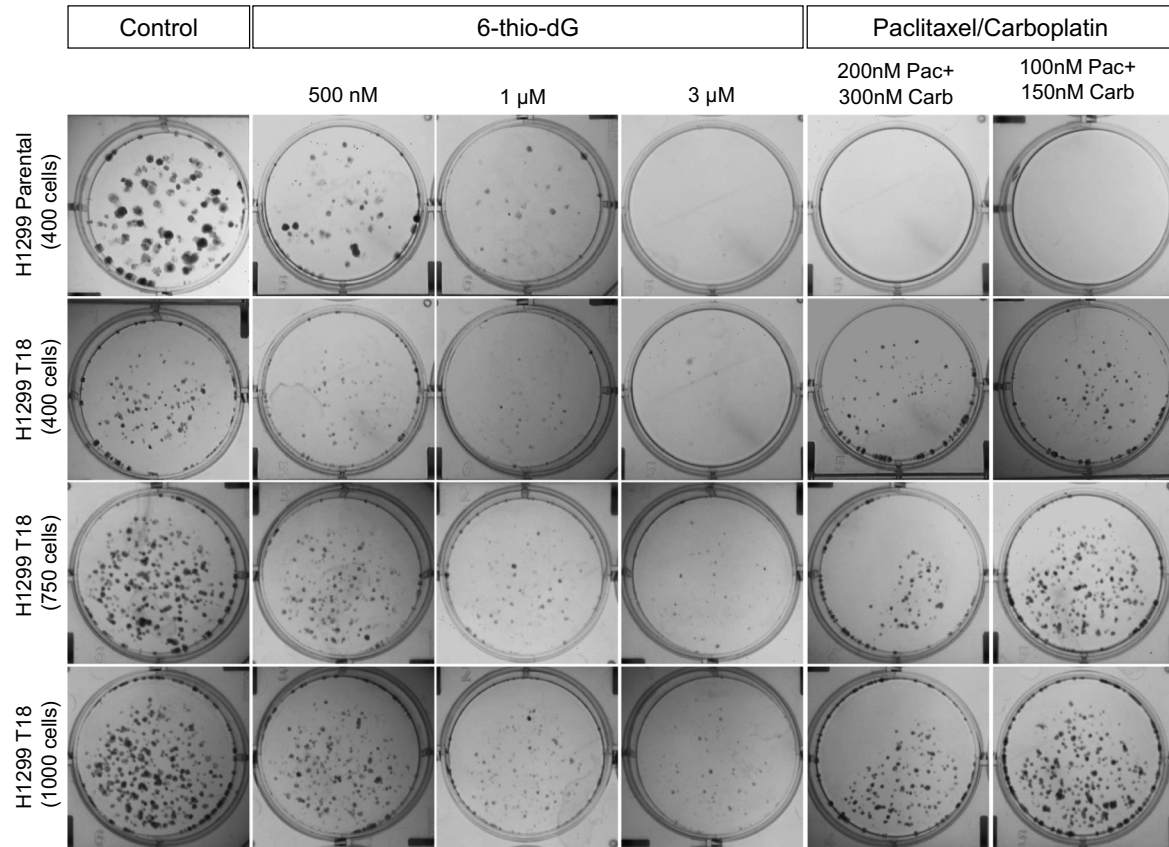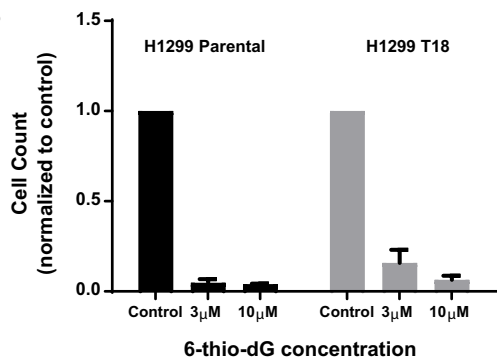
D

genetic heterogeneity. This clone was used to establish different PERCs [7].

In this study, we tested a subset of these erlotinib-resistant clones to determine if they were also resistant to 6-thio-dG. We seeded PERCs (PERC9, PERC10, PERC13, PERC16, and PC9-ER) into six-well plates cultured in erlotinib-containing medium. Previously, it was demonstrated that the resistance of PERC10, PERC13, and PERC16 to erlotinib was related to an increased ERK-pathway dependence. However, the resistance of PERC9 was linked to T790M-EGFR mutation, while PC9-ER is a polyclonal erlotinib-resistant cell line. We found that erlotinib-sensitive (PC9-1) and -resistant (PERC9, PERC10, PERC13, PERC16, and PC9-ER) clones all remained very sensitive (in the low nanomolar range) to 6-thio-dG irrespective of the mechanism of erlotinib acquired resistance (Figure 2, A-B and Supplementary Fig. S2, A-E). Additionally, we cultured PERC16 in erlotinib-free medium to compare with erlotinib-containing medium conditions and found that PERC16 clones were still sensitive to 6-thio-dG (30 nM) (data not shown). In another experiment, we tested a third-generation EGFR inhibitor osimertinib (selective for both TKI sensitizing and T790M resistance mutations) in PC9-1 and PERC9 clones to determine if erlotinib-sensitive PC9-1 and erlotinib-resistant PERC9 clones that harbor T790M mutation were sensitive to a next-generation EGFR inhibitor. We found that while the PC9-1 erlotinib-sensitive cells were also sensitive to 10 nM osimertinib (Supplementary Fig. S3A), the PERC9 erlotinib-resistant cells were resistant to 10-100 nM osimertinib (Figure 2C). Despite this resistance to erlotinib and osimertinib, PERC9 cells remained highly sensitive to 30 nM 6-thio-dG (Figure 2C). However, the results with 10, 30, and 100 nM osimertinib looked similar in PC9-1 cells, showing the non–dose-dependent effect of osimertinib in these cells. There are two possible explanations for the non–dose-dependent manner. The first explanation is that cells are not in logarithmic decline phase in between 10 nM and 100 nM concentration of osimertinib; they are in plateau phase. The second explanation is the presence of osimertinib resistance colonies in small subpopulation. Resistance can emerge from this small subpopulation, but it may require culturing these cells long term. In addition, we investigated the relationship between telomere length and sensitivity to 6-thio-dG, even though we previously found a lack of correlation between telomere length and 6-thio-dG sensitivity [14]. We performed the TeSLA to quantitate the average and shortest telomeres in the cells targeted with 6-thio-dG. We found that the average telomere length of PERC9, PERC13, and PERC16 erlotinib-resistant clones was longer and the percentage of the cells with telomeres shorter than 1.6 kb was less than the PC9-1 erlotinib-sensitive clone (Figure 2D). These results indicate that 6-thio-dG targets cells with both short and long telomeres equally, demonstrating that the cell-killing effect is independent of the initial

telomere length of the tumor cell as also demonstrated in the large NSCLC panel tested (Figure 1B).

In order to assess anticancer activity of 6-thio-dG in vivo, we used the erlotinib-sensitive (PC9-1) and -resistant (PERC16) clones to establish xenografts in nude mice. Based on our previous in vivo dose-defining results [14], 5 mg/kg of 6-thio-dG (i.p. and/or oral gavage) or 15 mg/kg erlotinib (oral gavage) was given daily. As expected, the PC9-1–derived group remained sensitive to erlotinib, whereas tumors continued to grow with erlotinib treatment in the erlotinib-resistant PERC16-derived group compared to control treatment groups (Figure 2, E and F). After 12 days of erlotinib treatment of PERC16 tumors, we provided 6-thio-dG (via oral gavage daily at 5 mg/kg) for an additional 1 week. This resulted in ~35% tumor shrinkage (Figure 2F). Thus, the resistant tumor growing in the presence of 15 mg/kg erlotinib remained sensitive to 6-thio-dG in vivo, demonstrating that 6-thio-dG results in drug-resistant tumor shrinkage.

To test the ability of 6-thio-dG to overcome chemotherapy resistance more broadly, we used H1299 NSCLC cells resistant to paclitaxel/carboplatin doublet therapy. The H1299 parental cells are sensitive to 100 nM paclitaxel combined with 150 nM carboplatin. These sensitive cells were treated with paclitaxel/carboplatin doublet therapy in clinically relevant doses for 8-9 months for 18 cycles (1 cycle: a drug on–drug off period) to develop resistant cell lines, as previously described [16]. The cells, termed H1299 T18, acquired a 53-fold increased resistance to paclitaxel/carboplatin chemotherapy. This resistance had two components: the first was the upregulation of ABC transporter expression leading to classical multidrug resistance. The second was the upregulation of KDM lysine demethylases [16]. It was this latter mechanism that resulted in these platin-taxane–resistant NSCLC cells to become exquisitely sensitive to KDM lysine demethylase (Jumonji) inhibitors [16]. We tested the effects of 6-thio-dG (1, 3, and 10 μM) on these sensitive and resistant isogenic H1299 cells and found that both the H1299 T18 NSCLC resistant cell and the parental H1299 cells remain sensitive to 6-thio-dG (Figure 3, A and B). We also performed the TeSLA assay for H1299 T18 paclitaxel/carboplatin-resistant cells and found that H1299 T18–resistant cells have shorter average telomere length (% of cells with <1.6 kb telomere length was higher) compared to H1299 parental (paclitaxel/carboplatin sensitive) cells (Figure 3C). In summary, H1299 T18 cells that demonstrated resistance to platin-taxane chemotherapy including both upregulation of expression of both ABC transporter and selected KDM demethylases remained sensitive to 6-thio-dG treatment.

In order to assess the anticancer activity of 6-thio-dG in vivo, we used the paclitaxel/carboplatin (H1299 T18)–resistant cells to establish xenografts in nude mice. We observed that 6-thio-dG (5 mg/kg, i.p., daily) significantly reduced the tumor growth rate in H1299 T18, whereas treatment with a vehicle control did not (Figure 3D). Thus, 6-thio-dG may be a valuable small molecule drug with minimal toxicities for reversing

Figure 3. (A) Colony formation assay of H1299 parental and paclitaxel:carboplatin-resistant cells at indicated doses for 11-13 days. Representative image of three biological replicates is shown for each experimental sample. (B) The cell counts of H1299 parental and H1299 T18 cells treated with 3 and 10 μM 6-thio-dG for 1 week (control; DMSO:water) (SDs from two to three independent experiments). (C) Results of TeSLA using DNA for H1299 parental and H1299 T18. Eight TeSLA PCRs (30 pg of each reaction) were performed for each DNA sample. TeSLA image quantification software was used to determine the average telomere length (Avg TL, kb), shortest 20% (kb), and <1.6 kb (%). P < .01, fold change >2. (D) Intraperitoneal injection of 6-thio-dG (5 mg/kg, daily) in H1299 T18–derived xenografts for 15 days. Control versus 6-thio-dG: P < .0001.
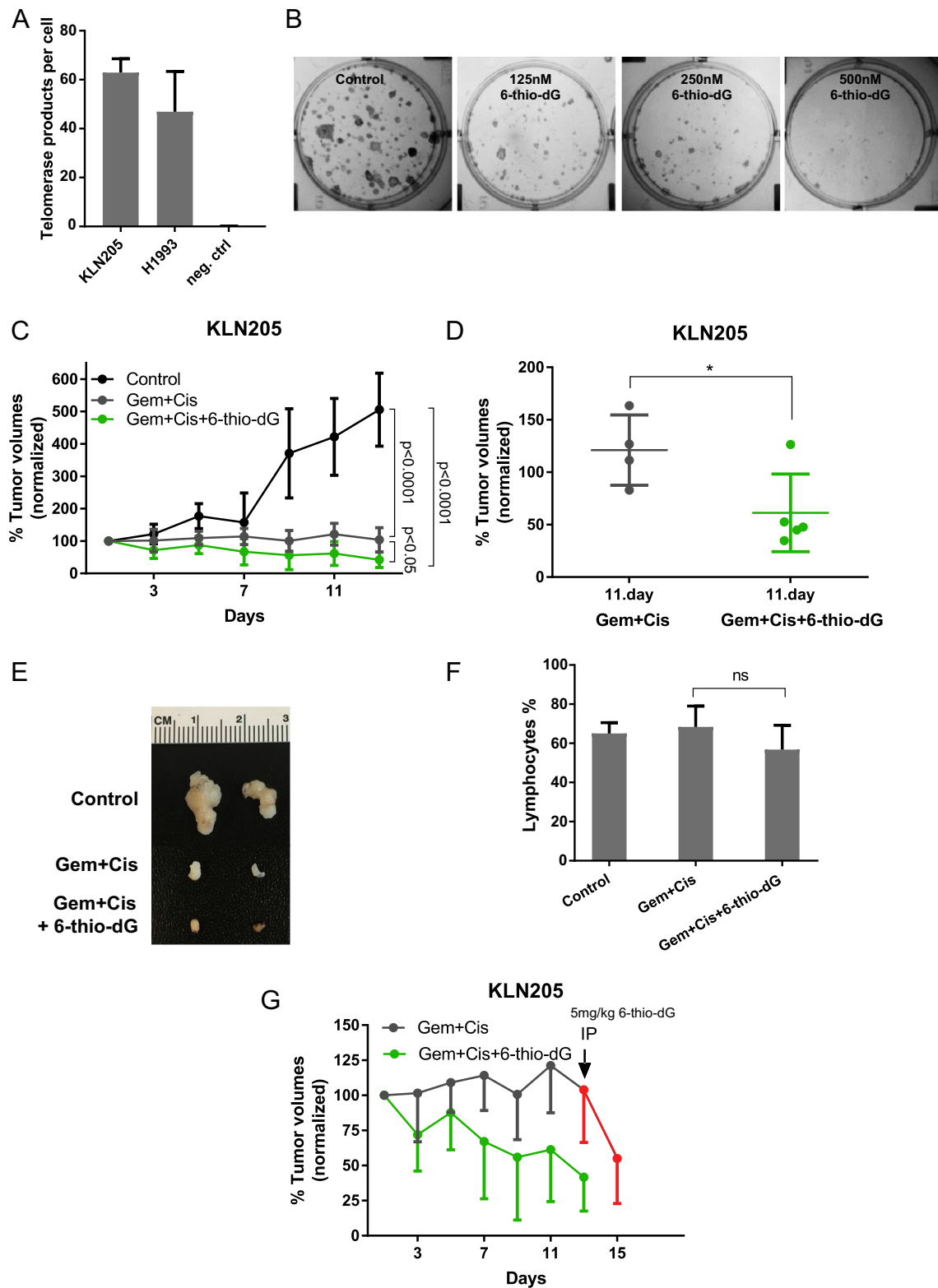
Figure 4. (A) Telomerase activity of KLN205 by using ddTRAP. H1993 NSCLC cell line is a positive control. (B) *In vitro* colony formation assay of KLN205 mouse lung tumor cells at indicated doses for 11-13 days. Cells were then fixed and stained with crystal violet. Representative image of three biological replicates are shown. (C) A syngeneic tumor mouse model in DBA/2 mice. 6-thio-dG: 2.5 mg/kg (oral gavage, daily), gemcitabine (Gem): 15 mg/kg (i.p., every 2-3 days), and cisplatin (Cis): 1 mg/kg (i.p., every 5-6 days) for 13 days. Control versus 6-thio-dG + Gem+Cis: $P < .0001$, control versus Gem+Cis: $P < .0001$. 6-thio-dG + Gem+Cis versus Gem+Cis: $P < .05$, ANOVA mixed-effect models. (D) Comparison of tumor volumes between Gem+Cis and Gem+Cis+6-thio-dG at day 11. (E) Representative tumor images (two tumors from each experimental group). (F) Percentage of total lymphocyte count shown following vehicle, Gem+Cis, and Gem+Cis+6-thio-dG. Gem+Cis versus Gem+Cis+6-thio-dG: $P = ns$, two-tailed unpaired t test. (G) The experimental group that was given Gem+Cis doublet therapy for 13 days was switched to 6-thio-dG alone (5 mg/kg, i.p.) at the end of treatment (red line).
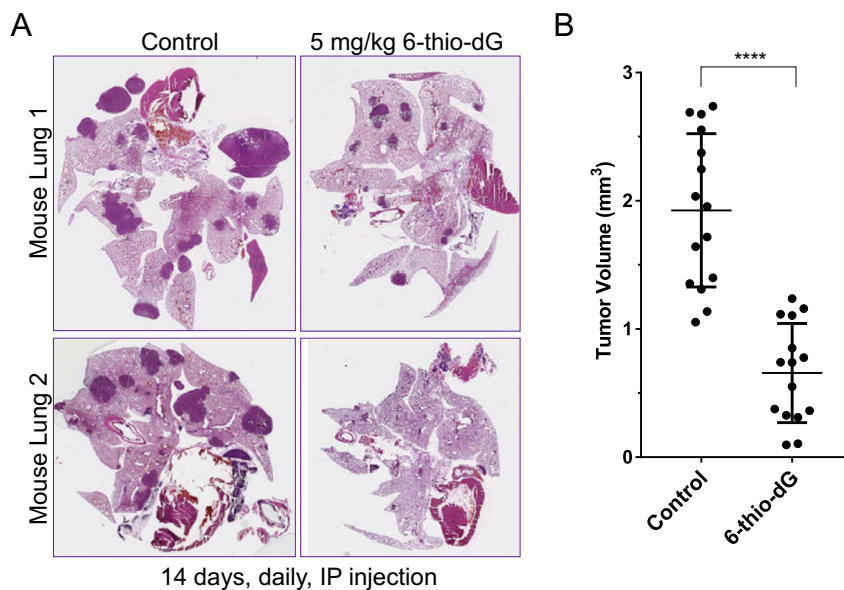
Figure 5. (A) H&E staining. Vehicle (5% DMSO) or 6-thio-dG (5 mg/kg) was injected into KRAS[LA1] strain mice (∼300 days old) for 14 days (daily, i.p.). Harvested lungs were analyzed for the number and volume of the tumors. Two representative mouse lungs are shown. (B) Tumor volumes (mm^3) of experimental groups (vehicle or 6-thio-dG treatment). Average tumor volumes were calculated from each H&E-stained lung section of five mice (3 sections per mouse). Each dot represents an average tumor volume of a section in mouse lung. Control versus 6-thio-dG: $P < .0001$, two-tailed unpaired t test.

or overcoming resistance to commonly used chemotherapeutic approaches.

6-thio-dG in Combination with Gemcitabine and Cisplatin Shrinks Tumors in an Immunocompetent Syngeneic Mouse Model

We next aimed to simulate clinical therapy with 6-thio-dG *in vivo* with combination therapy in the context of a functioning immune system. Since some immune cells transiently express telomerase and could therefore be potentially targeted by 6-thio-dG, we tested the effects of 6-thio-dG in a syngeneic (immunocompetent) tumor growth mouse model. Thus, we first tested 6-thio-dG *in vitro* on a mouse lung squamous cancer cell line, KLN205 [17], and found that the KLN205 telomerase-expressing cells (Figure 4A) were sensitive to 6-thio-dG in *in vitro* colony formation assays (Figure 4B). We introduced KLN205 cells into DBA/2 mice that have a fully competent immune system and are histocompatible with the allografted KLN205 tumor cell line. After establishing KLN205-derived tumors, we tested the anticancer activity of 6-thio-dG (2.5 mg/kg, oral gavage, daily), gemcitabine+cisplatin alone, and gemcitabine+cisplatin in combination with 6-thio-dG. We lowered 6-thio-dG concentration from 5 mg/kg to 2.5 mg/kg in this drug combination model and found that the percentage of tumor volumes of control, 6-thio-dG, gemcitabine+cisplatin, and gemcita-bine+cisplatin+6-thio-dG was ∼506%, ∼268% (not shown in graph), ∼104%, and 42% at the end of a 13-day treatment, respectively (percentage changes compared to the tumor volume in the control mice at a given day). Thus, while the combination of gemcitabine and cisplatin partially inhibited progressive tumor growth, it did not shrink the tumor. The addition of 6-thio-dG together with the gemcitabine and cisplatin combination led to ∼50% tumor shrinkage (Figure 4, C-E). Importantly, total lymphocyte counts did not change between mouse groups during the 13-day treatment

period (Figure 4F); however, we did observe a small weight loss in 6-thio-dG + Gem+Cis compared to control (this difference is significant with ANOVA). Thus, combining 6-thio-dG with first-line lung cancer therapy was effective in this mice model. Finally, to determine if 6-thio-dG can overcome initial KLN205 gemcitabine+-cisplatin resistance, on day 13, we switched treatment from gemcitabine+cisplatin which had no effect on KLN205 tumor growth to treatment with 6-thio-dG alone (5 mg/kg, i.p), and the trend showed rapid tumor shrinkage but lacked statistically significance due to inadequate tumor sample (Figure 4G). Thus, in a preclinical model of "front-line" lung cancer chemotherapy, a syngeneic lung squamous cancer model shows dramatic responses to the combination of 6-thio-dG and gemcitabine+cisplatin *in vitro* and *in vivo*.

6-thio-dG Reduces Tumor Size in a KRAS Mutant Genetically Engineered Mouse Model (KRAS[LA1]) of Lung Cancer

We assessed the anticancer effects of 6-thio-dG in a genetically engineered mouse model (KRAS[LA1]) that carries oncogenic alleles of KRAS (G12D) activated by spontaneous recombination events which recapitulate the spontaneous oncogene activation as seen in human cancer in the presence of an intact immune system [20]. In a pilot experiment with 300-day-old mice with significant tumor burden, we observed a 66% reduction in tumor volume with 6-thio-dG treatment (i.p., daily, 5 mg/kg, 14 days) and did not observe weight loss between mouse groups during the treatment period (Figure 5).

Discussion

Chemotherapy and/or targeted therapies for advanced NSCLC often provide partial antitumor responses in patients but almost universally are associated with subsequent tumor recurrences requiring additional treatments in the second- and third-line setting. It appears that tumor

cells remaining after primary therapy persist in a "drug-tolerant" ("persister") state for weeks to months and then move to a "drug-resistant" state [24, 25]. Due to tumor cell heterogeneity/plasticity, a single tumor cell can expand and emerge with diverse therapy resistance mechanisms. Thus, some drug-resistant "persisters" will respond to additional therapy, while other "persisters" will not [7]. Therefore, it is important to identify therapies that work across resistant/persister cell phenotypes to provide patients with durable long-lasting remissions.

In our previous study, we described the nucleoside analogue 6-thio-dG as a potential therapeutic agent and demonstrated its mechanism of action. 6-thio-dG affected telomerase-positive cancer cells but had minimal toxicity to long-term–treated mice and to telomerase-negative normal human colonic epithelial and fibroblast cells [14]. We also showed that targeting telomerase with 6-thio-dG overcame therapy resistance in pediatric brain tumors (demonstrating that 6-thio-dG can cross the blood brain barrier) [24]. In addition, we demonstrated sensitivity to 6-thio-dG in BRAF and checkpoint inhibitor–resistant melanomas [22, 23]. Here in this study, we extended our preclinical studies to more clinically relevant lung cancer model systems. Thus, we tested the anticancer effect of 6-thio-dG on first-line EGFR tyrosine kinase inhibitor targeted therapy– or platin-taxane chemotherapy–resistant NSCLC cells. Although the fraction of the oral administered 6-thio-dG that reaches systemic circulation or the tumor was not investigated in this study, here for the first time, we demonstrate the efficacy of 6-thio-dG through oral administration.

We used three different *in vivo* models to demonstrate that 6-thio-dG is effective in overcoming lung cancer drug resistance to EGFR targeted therapy and platin-doublet chemotherapy. Two of the human lung cancer preclinical models (erlotinib-resistant EGFR mutant NSCLCs and paclitaxel/carboplatin-resistant NSCLCs) showed sensitivity in xenografted tumors to 6-thio-dG delivered orally or by i.p. injection with significant tumor shrinkage. We also tested the effects of 6-thio-dG in a syngeneic mouse tumor model with intact immunity as a third *in vivo* model. Since some proliferating immune cells transiently express telomerase, there was the possibility that 6-thio-dG could have reduced T-cell–mediated antitumor effects. We used the KLN205 mouse cancer cell line in DBA/2 mice since this is a well-established model of combining gemcitabine and cisplatin's efficacy and safety [26]. When we combined 6-thio-dG with gemcitabine and cisplatin, we observed an additional ~50% reduction in tumor volume compared to gemcitabine and cisplatin combination therapy alone over a 13-day treatment period. In addition, we demonstrated that adding 6-thio-dG treatment to a KLN205 tumor not responding to gemcitabine+cisplatin therapy resulted in further dramatic tumor shrinkage. We saw no correlation in NSCLCs with response to 6-thio-dG and tumor telomere length. In addition, the KLN205 experiments showed that 6-thio-dG works in mouse tumors that have relatively long telomeres.

Finally, we showed that 6-thio-dG treatment resulted in significant tumor reduction in a genetically engineered mutant KRAS model of lung adenocarcinoma again with an intact immune system. In addition, in the xenograft and GEMM experiments, we did not observe weight loss during the treatment, and the total lymphocyte count did not change by adding 6-thio-dG to the gemcitabine+cisplatin therapy. This is consistent with our previous studies showing less toxicity of 6-thio-dG alone in wild-type mice up to 25 days (lack of weight loss; no changes in hematological, renal, or liver functions) [14].

There is an urgent clinical need for effective therapeutic targets to reverse drug resistance. In the current study, we provide compelling preclinical evidence of significant efficacy of 6-thio-dG in a variety of NSCLC clinical settings as a first-line therapy as a single agent or in combination with conventional therapies, or in the maintenance setting. In summary, 6-thio-dG is a highly promising telomerase-mediated telomere-targeted therapy for NSCLC that has activity in untreated cancers and in NSCLCs with resistance to either targeted therapy or platin-doublet chemotherapy. These findings support the further investigation of candidate biomarkers, which predict sensitivity to 6-thio-dG and could be translated into the clinic by identifying a biomarker-defined patient population that would receive greater benefit from 6-thio-dG.

Author Contributions

I. M. designed and performed experiments, analyzed data, and wrote the initial manuscript. R. L. helped with *in vivo* experiments and edited the manuscript. K. L. and W. D. helped with *in vivo* experiments. M. P. helped in performing CellTiter-Glo assays. C. C. helped with cell culture, and K. B. helped with statistical analysis. T. L. performed the TeSLA assay. M. R., M. D., R. B., E. D. M., J. D. M., L. F. W., and S. J. A. provided the cell lines and edited the manuscript. W. E. W. edited the manuscript. J. W. S. designed and guided the project and co-wrote the manuscript.

Acknowledgements

Appendix A. Supplementary data

Supplementary data to this article can be found online at https://doi.org/10.1016/j.neo.2018.06.002.

References

[1] Siegel RL, Miller KD, and Jemal A (2017). Cancer statistics, 2017. *CA Cancer J Clin* **67**, 7–30.

[2] Zhang W, Lei P, Dong X, and Xu C (2014). The new concepts on overcoming drug resistance in lung cancer. *Drug Des Devel Ther* **8**, 735–744.

[3] Rossi A, Chiodini P, Sun JM, O'Brien ME, von Plessen C, Barata F, Park K, Popat S, Bergman B, and Parente B, et al (2014). Six versus fewer planned cycles of first-line platinum-based chemotherapy for non–small-cell lung cancer: a systematic review and meta-analysis of individual patient data. *Lancet Oncol* **15**, 1254–1262.

[4] Ramos P and Bentires-Alj M (2015). Mechanism-based cancer therapy: resistance to therapy, therapy for resistance. *Oncogene* **34**, 3617–3626.

[5] Piotrowska Z and Sequist LV (2016). Treatment of EGFR-mutant lung cancers after progression in patients receiving first-line EGFR tyrosine kinase inhibitors: a review. *JAMA Oncol* **2**, 948–954.

[6] Ayeni D, Politi K, and Goldberg SB (2015). Emerging agents and new mutations in EGFR-mutant lung cancer. *Clin Cancer Res* **21**, 3818–3820.

[7] Ramirez M, Rajaram S, Steininger RJ, Osipchuk D, Roth MA, Morinishi LS, Evans L, Ji W, Hsu CH, and Thurley K, et al (2016). Diverse drug-resistance mechanisms can emerge from drug-tolerant cancer persister cells. *Nat Commun* **7**10690.

[8] Syn NL, Teng MWL, Mok TSK, and Soo RA (2017). De-novo and acquired resistance to immune checkpoint targeting. *Lancet Oncol* **18**, e731–e741.

[9] Kim NW, Piatyszek MA, Prowse KR, Harley CB, West MD, Ho PL, Coviello GM, Wright WE, Weinrich SL, and Shay JW (1994). Specific association of human telomerase activity with immortal cells and cancer. *Science* **266**, 2011–2015.

[10] Shay JW and Bacchetti S (1997). A survey of telomerase activity in human cancer. *Eur J Cancer* **33**, 787–791.

[11] Chiappori AA, Kolevska T, Spigel DR, Hager S, Rarick M, Gadgeel S, Blais N, Von Pawel J, Hart L, and Reck M, et al (2015). A randomized phase II study of the telomerase inhibitor imetelstat as maintenance therapy for advanced non–small-cell lung cancer. *Ann Oncol* **26**, 354–362.

[12] Shay JW (2016). Role of telomeres and telomerase in aging and cancer. *Cancer Discov* **6**, 584–593.

[13] Frink RE, Peyton M, Schiller JH, Gazdar AF, Shay JW, and Minna JD (2016). Telomerase inhibitor imetelstat has preclinical activity across the spectrum of non–small cell lung cancer oncogenotypes in a telomere length dependent manner. *Oncotarget* **7**, 31639–31651.

[14] Mender I, Gryaznov S, Dikmen ZG, Wright WE, and Shay JW (2015). Induction of telomere dysfunction mediated by the telomerase substrate precursor 6-thio-2′-deoxyguanosine. *Cancer Discov* **5**, 82–95.

[15] Mender I, Gryaznov S, and Shay JW (2015). A novel telomerase substrate precursor rapidly induces telomere dysfunction in telomerase positive cancer cells but not telomerase silent normal cells. *Oncoscience* **2**, 693–695.

[16] Dalvi MP, Wang L, Zhong R, Kollipara RK, Park H, Bayo J, Yenerall P, Zhou Y, Timmons BC, and Rodriguez-Canales J, et al (2017). Taxane-platin–resistant lung cancers co-develop hypersensitivity to JumonjiC demethylase inhibitors. *Cell Rep* **19**, 1669–1684.

[17] Kaneko T, LePage GA, and Shnitka TK (1980). KLN205—a murine lung carcinoma cell line. *In Vitro* **16**, 884–892.

[18] Ludlow AT, Robin JD, Sayed M, Litterst CM, Shelton DN, Shay JW, and Wright WE (2014). Quantitative telomerase enzyme activity determination using droplet digital PCR with single cell resolution. *Nucleic Acids Res* **42**e104.

[19] Mender I and Shay JW (2015). Telomere dysfunction induced foci (TIF) analysis. *Bio Protoc* **5**.

[20] Johnson L, Mercer K, Greenbaum D, Bronson RT, Crowley D, Tuveson DA, and Jacks T (2001). Somatic activation of the K-ras oncogene causes early onset lung cancer in mice. *Nature* **410**, 1111–1116.

[21] Lai TP, Zhang N, Noh J, Mender I, Tedone E, Huang E, Wright WE, Danuser G, and Shay JW (2017). A method for measuring the distribution of the shortest telomeres in cells and tissues. *Nat Commun* **8**, 1356.

[22] Sengupta S, Sobo M, Lee K, Senthil Kumar S, White AR, Mender I, Fuller C, Chow LM, Fouladi M, and Shay JW, et al (2018). Induced telomere damage to treat telomerase expressing therapy-resistant pediatric brain tumors. *Mol Cancer Ther* . https://doi.org/10.1158/1535-7163. MCT-17-0792.

[23] Zhang G, Wu LW, Mender I, Barzily-Rokni M, Hammond MR, Ope O, Cheng C, Vasilopoulos T, Randell S, and Sadek N, et al (2018). Induction of telomere dysfunction prolongs disease control of therapy-resistant melanoma. *Clin Cancer Res* . https://doi.org/10.1158/1078-0432. CCR-17-2773.

[24] Sharma SV, Lee DY, Li B, Quinlan MP, Takahashi F, Maheswaran S, McDermott U, Azizian N, Zou L, and Fischbach MA, et al (2010). A chromatin-mediated reversible drug-tolerant state in cancer cell subpopulations. *Cell* **141**, 69–80.

[25] Banelli B, Carra E, Barbieri F, Wurth R, Parodi F, Pattarozzi A, Carosio R, Forlani A, Allemanni G, and Marubbi D, et al (2015). The histone demethylase KDM5A is a key factor for the resistance to temozolomide in glioblastoma. *Cell Cycle* **14**, 3418–3429.

[26] Kaneko T and LePage GA (1978). Growth characteristics and drug responses of a murine lung carcinoma in vitro and in vivo. *Cancer Res* **38**, 2084–2090.